Soft Matter

Cite this: *Soft Matter*, 2012, **8**, 2070

www.rsc.org/softmatter

REVIEW

Extreme wettability and tunable adhesion: biomimicking beyond nature?

Xinjie Liu,[ab] Yongmin Liang,[a] Feng Zhou*[a] and Weimin Liu[a]

Received 20th October 2011, Accepted 3rd November 2011
DOI: 10.1039/c1sm07003g

In this critical review, we summarize the recent developments of extreme wettability in nature and biomimetic examples, and then we focus on surface wetting behavior beyond nature, which means surface wetting properties that cannot be found in nature. They are: switchable wettability between (super)hydrophobicity and (super)hydrophilicity, switchable water/oil droplet adhesion between superhydrophobic pinning states and superhydrophobic rolling states, superoleophobicity at the air–solid interface or even under vacuum, and self-healing (super)amphiphobicity at the air–solid interface.

Introduction

Nature has provided us with luxuriant surfaces and interface resource pools with diverse wettabilities from superhydrophilicity to superhydrophobicity (two extremes) found in plant leaves[1–3] (most typically lotus leaves), feathers of birds,[4,5] legs/back/wings of insects[6–8] and silk of spiders.[9] These possess properties of self-cleaning by minimizing the water and contaminant adhesion, or pinning spherical water droplets, collecting water droplets by integrating water vapor collection and droplet transportation. Besides, natural candidates can preserve their surface properties very well due to the self-healing function. Biomimicking these fascinating surfaces has been one of the most active research topics in the past few years and it has been reviewed in a number of publications.[10–18]

Surfaces with superhydrophobicity are usually fabricated by first forming hierarchical micro/nanoscale binary structures and afterwards chemical modification with low surface energy materials. The apparent surface wettability existing in nature can be simply mimicked by following this principle. With the expanded use of different coating materials, in particular, smart materials responsive to photo, thermal, pH, electro potential, electrolytes *etc.*, some surface properties not observed in nature can be achieved, for instance, switchable wettability whereby a surface behaves (super)hydrophobic under some circumstances and (super)hydrophilic in other cases, switchable water droplet adhesion between a superhydrophobic pinning state and

[a]*State Key Laboratory of Solid Lubrication, Lanzhou Institute of Chemical Physics, Chinese Academy of Sciences, Lanzhou, 730000, P. R. China. E-mail: zhouf@lzb.ac.cn*
[b]*Graduate College of Chinese Academy of Sciences, Beijing, 100083, P. R. China*

Xinjie Liu

Xinjie Liu is currently a PhD student at Lanzhou institute of Chemical Physics, Chinese Academy of Sciences (LICPCAS). He received his BSc degree in Sichuan University, China in 2006. In 2006, he was given permission to be exempted from tests to be a M.D. and Ph. D. combined program of Chinese Academy of Science to join Prof. Feng Zhou's group at LICPCAS. In 2011, he is awarded the scholarship of "Outstanding President Award of Chinese Academy of Science". His current research interests are focused on materials with special wettability and adhesion behavior and the corresponding mechanism study.

Yongmin Liang

Professor Yongmin Liang received his B.S. degree in chemistry from Shanxi Normal University (1989), and M.S. degree (1992) and PhD (1998) from Lanzhou University. After his postdoctoral research experience at Tinghua University (Taiwan), he joined the faculty of Lanzhou Institute of Chemical Physics under the name of "Top Hundred Talents" Program at the Chinese Academy of Sciences (2002). He is also a professor of College of Chemistry, Lanzhou University. His research interests include homogeneous catalysis and organomaterials synthesis.

superhydrophobic rolling state, superoleophobicity at the air–solid interface or even under vacuum, and self-healing wettability. "Inspired by nature, but achieving surface properties that nature doesn't have", we just call this "biomimicking beyond nature". This critical review firstly mentions typical examples found in nature and the brief progress on biomimicking, followed by a detailed presentation of "biomimicking beyond nature" in the following four aspects: smart surfaces with reversible switchable wettability, smart surfaces with reversible switchable liquid droplet adhesion, superoleophobicity in air and under vacuum and self-healing superamphiphobicity (Scheme 1). Finally some perspectives on future developments are discussed.

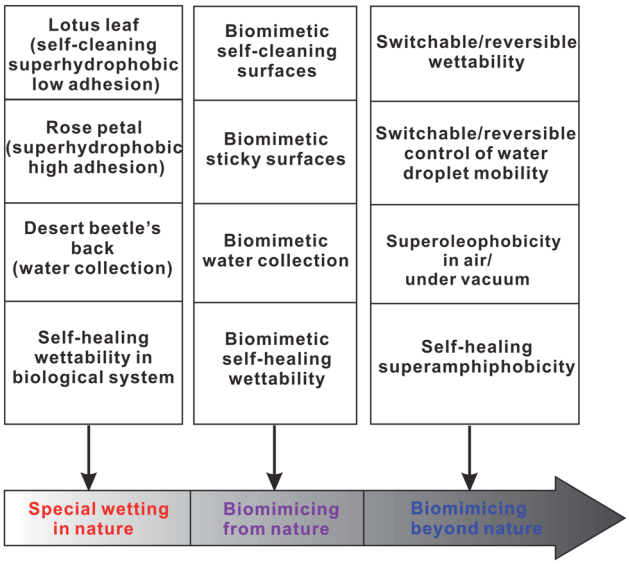

Scheme 1 An overview of the special wettability in nature and biomimicking wettability from nature and beyond nature.

1 Extreme wettability: from natural to bio-inspired surfaces

1.1 Superhydrophobic surfaces

Early in 1996, Onda *et al.* reported super-water-repellent fractal surfaces by low surface energy materials on rough surfaces.[10] Afterwards, Barthlott and Neinhuis,[3,4] revealed the self-cleaning mechanism of a lotus leaf (Fig. 1A–C) as a result of the large water contact angle (CA > 150°) and the small sliding angle (SA) of less than 5° (low contact angle hysteresis) so that water droplets slide very easily on the surface and so carry off contaminant particles. The lotus surface is constituted of micro/nano scale binary structures (nano scale tubular structures distributed on micro scale papillae structures), that are covered by epicuticular wax. The combination results in superhydrophobic properties (high water CA and low SA) and is the basic principle of biomimicking extreme wettability.[12–18] Superhydrophobicity or super-water repellency (ultra-hydrophobicity) means that a water contact angle on a certain surface is bigger than 150°. Water droplets can slide or be pinned on superhydrophobic surfaces, which are denoted as the "lotus effect" or the "rose petal effect" and their difference will be discussed in detail in section 1.2.

Except for the lotus leaf, many other plant-leaves also possess superhydrophobic properties such as the rice leaf, taro leaf, India canna, purple setcreasea, watermelon leaf, ramee leaf, perfoliate knotweed and lady's mantle leaf.[2,4,13] In addition to plant leaves, some parts of many insects also possess superhydrophobicity, such as the legs of the water strider,[6] the wings of a butterfly[21] and cicadas.[22] Water striders can easily walk on water relying on their non-wetting legs (Fig. 1D–F). The maximum supporting weight of a single leg can be about 15 times the weight of the water strider itself.[6] The superhydrophobicity found on Cicadaes' wings, duck feathers,[4] the superhydrophobic eyes of mosquitoes[23] and natural plastrons of some animals or insects[24,25] all

Feng Zhou

Professor Feng Zhou is a Professor at the State Key Lab of Solid Lubrication, Lanzhou Institute of Chemical Physics under the name of "Top Hundred Talents" Program of Chinese Academy of Sciences. He got his PhD in 2004 at the Lanzhou Institute of Chemical Physics. He spent three years (2005–2008) in the Department of Chemistry, University of Cambridge as a postdoctoral research associate. He has published more than 100 journal papers. His research interests are micro/nanostructured surfaces for lubrication, drag/noise reduction and anti-biofouling applications, and high performance lubricants.

Weimin Liu

Professor Weimin Liu got his PhD in 1990 at the Lanzhou Institute of Chemical Physics. Currently, he is a full professor and director of the Lanzhou Institute of Chemical Physics, Chinese Academy of Sciences, and the director of the State Key Laboratory of Solid Lubrication. His research interests cover organic and nanoparticular lubricating oil additives, synthetic lubricants and space tribology. He is the chief scientist of China "973" project on "Fundamental Research of Lubricating and Antiwear Materials under Extreme Operating Conditions" and the leading scientist of the most recent space tribology program of China at SZ-7 Spacecraft. He has published over 400 journal papers and gained a number of national scientific awards.

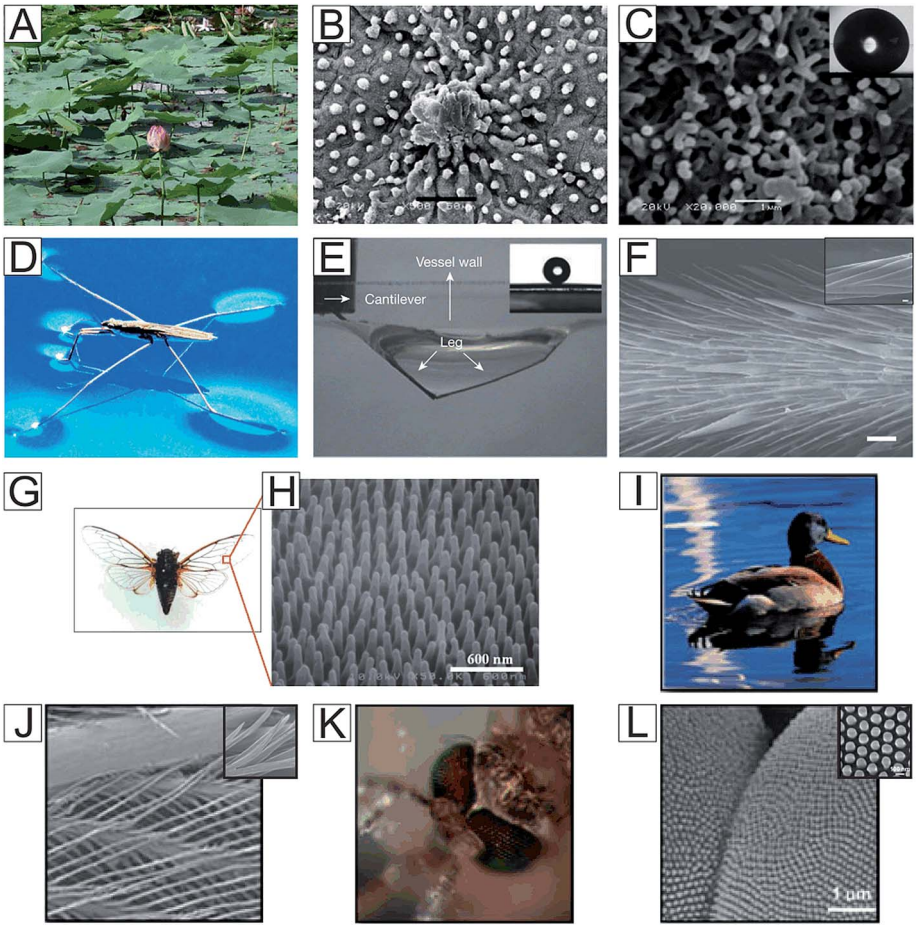

Fig. 1 (A–C) Photos of some lotus leaves on a pond and the corresponding SEM images of lotus leaves with different magnifications. (D–F) Photograph of a water strider standing on the water surface and the corresponding SEM images. (G–H) Digital pictures of cicada orni and the FE-SEM image of its wing's surface nanostructure. (I–L) The digital and corresponding SEM images of duck feather and mosquito eye, respectively.

comes from the ordered surface structures and low surface energy coatings on top (Fig. 1G–L). These components possess self-cleaning properties, and therefore they are all empirically ascribed to the category of "lotus effects".

Inspired by the lotus effect, a great variety of artificial superhydrophobic self-cleaning surfaces have been fabricated. For example, Jiang *et al.* reported a superhydrophobic surface resembling the surface morphology of a lotus leaf (Fig. 2A).[26] Approaches to form complex surface morphologies with dual scale structures have been vastly developed depending on material types to be modified, including light irradiation,[27] solvent evaporation,[28] wet chemical etching,[29,30] plasma polymerization,[31–34] sublimation,[35] sol–gel method,[36–38] chemical vapor deposition,[39,40] anodic oxidation,[41,42] microfabrication,[43–45] mechanical action[46] and electro-synthesis (for example, electropolymerization Fig. 2B)[47] or electrodeposition[48,49] *etc*. To mimic the morphology of nature's examples, replication using sample surfaces from nature as templates is the most direct way. For instance, Koch *et al.* replicated surface structures of the lotus leaf and afterwards assembled the natural lotus wax on the surfaces by thermal evaporation to obtain superhydrophobic surfaces with low adhesion (Fig. 2C).[50] For superhydrophobic surfaces to be used in practice, both the surface structure and modification

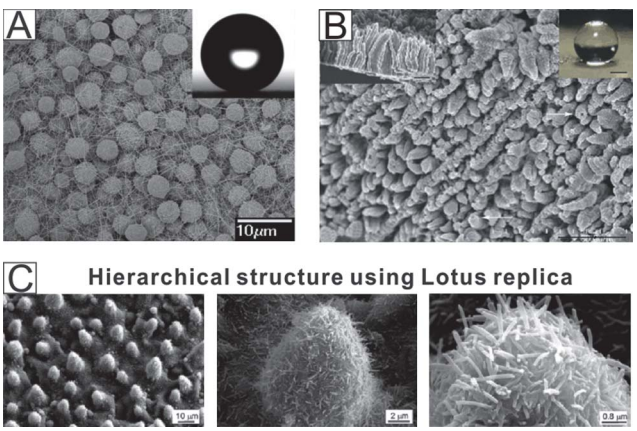

Fig. 2 (A) SEM images of superhydrophobic polystyrene films with special microsphere/nanofiber composite structures prepared *via* the EHD method. (B) SEM image of an aligned poly(alkylpyrrole) microtube film prepared *via* the ECD method. The inset shows a water droplet on the film (scale bar: 500μm). (C) Hierarchical structure using a lotus leaf. Nano- and hierarchical structures were fabricated with a mass of 0.8 mg mm^{-2} of Lotus wax after storage for seven days at 50 °C with ethanol vapor.

coatings must be robust enough, and they must be suitable for mass production as well. These surfaces must resist abrasive friction and contamination, and their mechanical robustness is of primary concern.[14,51,52] Apparently, most post modifications, where a thin layer of perfluorinated compounds is used, might not match the requirement as the coating materials are liable to be scratched off. Bell *et al.* reported that the discs made from compressed metal powders pre-modified by alkylthiol can maintain superhydrophobicity even after surface abrasion.[53] Another way relies on implementing complex structures into low surface energy bulk materials so that damage of the top surface layer won't affect the surface properties. For example, very complex micro/nanostructures on anodized alumina can be imprinted into polymeric coatings and materials, such as silicone elastomers, polyurethane, ultra-high-molecular-weight polyethylene and polytetrafluoroethylene *etc.* The as-prepared replicas exhibited superhydrophobicity even without further modification with low-surface-energy coatings.[54]

Surface coatings that can be produced with the industrially compatible approaches, for example spraying, brushing *etc.*, would be more practical in real applications, especially for those surface coatings made with cheap materials, simple fabrication procedures, and most importantly with the easy repairability. As a typical example, Wu *et al.* reported a simple, low-cost, and nontoxic method to prepare superhydrophobic coatings by spraying an alkane carboxylate emulsion solution on virtually any substrates and curing at ambient environment, which upon damaging can be easily repaired by local spraying.[55]

1.2 Superhydrophobic surfaces with high adhesive forces

Although most superhydrophobic surfaces show very low surface adhesion to water droplets (low contact angle hysteresis), sticky superhydrophobicity (superhydrophobicity with high sliding angle due to high CA hysteresis) does exist in nature, and the contact mode of sliding superhydrophobicity and sticky superhydrophobicity is different. Their difference can be explained by Wenzel (eqn 1) and Cassie equation (eqn 2):[19,20]

$$\cos\theta^* = r\cos\theta \quad (1)$$

$$\cos\theta^* = -1 + \phi_s(\cos\theta + 1) \quad (2)$$

where θ^* is the apparent contact angle for a droplet on a surface, θ is the Young's contact angle on an ideally flat surface with similar chemistry, r is the surface roughness which means the ratio of the actual area of a rough surface to the projected area, and ϕ_s is the fraction of solid–liquid contact.

CAH is the difference between advancing contact angle (θ_{adv}) and receding contact angle (θ_{rec}), and the value of CAH is finally determined by the contact mode. However, the advancing contact angles of superhydrophobic surfaces no matter in Wenzel state, Cassie state or metastable Cassie state (transition state from Cassie state to Wenzel state) show no big difference, because they are all bigger than 150° and less than 180°. Thus, the CAH is finally determined by receding angles which may be as low as 40° for superhydrophobic surfaces in the Wenzel state.[20] The magnitude of the CAH or adhesion force of a droplet on a superhydrophobic surface descends in the order "Wenzel state" > "metastable Cassie state" > "Cassie state". For sticky superhydrophobicity (Wenzel state and metastable Cassie state), the astriction of surface asperities for the liquid fraction left in the textures (such as capillary action of substrate with porous micro/nano scale structures) and surface chemistry of solid surface (such as hydrophilic interaction) lead to a high CAH,[12] because it is pure liquid–solid contact (area-contact) for the interface of the Wenzel model and line contact or point-contact for the interface of the metastable Cassie state. However, the astriction of surface asperities or surface chemistry for liquid droplet in Cassie state (sliding superhydrophobicity) is much smaller than that in the Wenzel state or metastable Cassie state (sticky superhydrophobicity), because the droplet is in contact with the air–solid composite interface in the Cassie state (point-contact), and there is a stable liquid bridge formed in the contact interface leading to low CAH. Detailed examples will be discussed in the following part.

Rose petals show not only superhydrophobicity but also high water droplet adhesion and this effect is defined as the "petal effect"[56] (Fig. 3A and B). It is demonstrated that both the micro-scale and nano-scale structures are larger than that of lotus leaves, therefore water droplets can easily penetrate into these larger grooves, leading to high capillary force and high adhesion force. Although we do not clearly know the actual function of the "rose petal effect" in nature, it might be very useful in manipulating droplet mobility in components of artificial devices. Inspired by the sticky superhydrophobicity of rose petals, Jiang *et al.* have prepared a densely packed and aligned PS nanotube film that shows high adhesion superhydrophobicity as shown in Fig. 3C and D.[57] Guo *et al.* fabricated an adhesive superhydrophobic engineering aluminum alloy surface composed of micro-orifices and nano-particles (Fig. 3E).[58] Lai *etc.* reported a superhydrophobic spongelike nanostructured TiO_2 film with controllable adhesion by modulating the hydrophobic/hydrophilic components on the substrate.[59] Very recently, they reported that water adhesion could also be manipulated by changing the nano-pore or nano-tube size of superhydrophobic TiO_2 substrate.[60] Capillary forces between the droplet and surface micro/nanostructures might be the main reason for high adhesion, where droplets wet the surfaces in a mixed Cassie and Wenzel mode (Fig. 3F).

Besides the surface topography induced wetting mode transition, the surface chemistry may also play a key role in inducing high droplet adhesion. When a small fraction of hydrophilic poly (styrene sulfonic acid) sodium salt (PSSNa) was embedded on the surface of rough PDMS replicas, the surface became both superhydrophobic and sticky (Fig. 3G). After ultrasonic removal of PSSNa, the surfaces became slippery and showed extremely low adhesion to water droplets, indicating a solvation force between the surface embedded polymer molecules and a droplet contributes to adhesion enhancement.[54] Ishii *et al.* fabricated a hybrid biomimetic surface consisting of hydrophilic metal domes and hydrophobic polymer spikes and demonstrated the "affinity driven adhesion" between water and hydrophilic metal domes.[61] The water droplet adhesion on the hybrid surface could be controlled by not only varying the dome density but also by the application of thermal treatment.

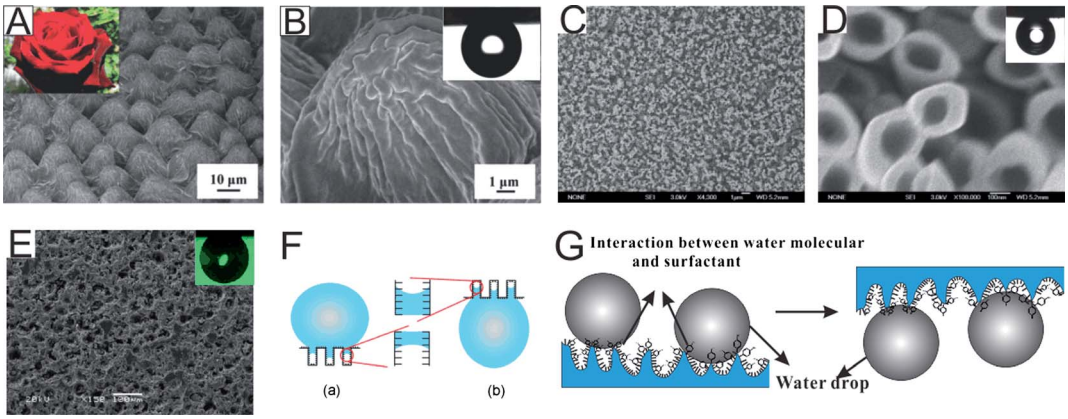

Fig. 3 (A,B) SEM images of the surface of a red rose petal, showing a periodic array of micropapillae and nanofolds on each papillae top; FE-SEM images of (C) top view of the aligned PS nanotube layer; (D) magnified image of C (in the inset, the shape of a water droplet on the PS surface when it is turned upside down); (E) the as-prepared etched aluminum alloy surface with a complementary structure to a lotus leaf (in the inset, the photo of a water droplet suspended on the as-prepared surface at the tilted 180°); (F) schematic illustration of the capillary force induced high adhesion. (G) Schematic illustration of the mechanism of nanoscale interactions between the water droplets and surfaces (water droplets pinning on a superhydrophobic surface by molecular anchors).

1.3 Patterned wetting for water collection

Some beetles (Fig. 4A) in the Namib desert collect water from fog-laden wind on their backs. The water collection mechanism is based on the insect's bumpy surface, which consists of alternating hydrophobic and hydrophilic regions. Droplets accumulate on the top (front) fused 'wings' (elytra) and roll down the beetle's surface to its mouthparts. The water in the fog settles on the peaks, forming fast-growing droplets that bind to the elytra; water striking the hydrophobic slopes can also be collected in a hydrophilic region. Each attached droplet eventually reaches a size at which its contact area covers the entire hydrophilic island. Beyond this size, the weight of the accumulated water droplet can overcome the capillary force that attaches it to the surface, and therefore the droplet detaches and rolls down the tilted hydrophobic path on the beetle's surface leading to its mouth (Fig. 4B). Parker *et al.* have mimicked the back of the Stenocara beetle to harvest water by fabricating hydrophilic bumps on hydrophobic wax films.[7]

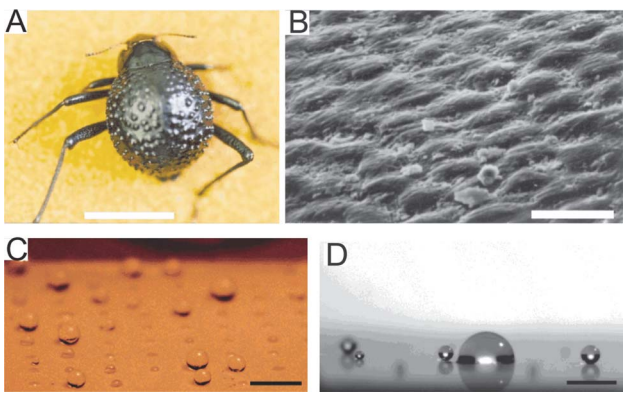

Fig. 4 The water-capturing surfaces of desert beetle (elytra) (A, Scale bar = 10 mm), scanning electron micro-graph of the textured surface of the depressed areas (B, Scale bar = 10 μm). (C) Small water droplets sprayed on a (PAA/PAH/silica nanoparticle/semi-fluorosilane) superhydrophobic surface with an array of hydrophilic domains patterned with a 1% PAA water/2-propanol solution (scale bar = 5 mm). (D) Sprayed small water droplets accumulate on the patterned hydrophilic area shown in (C) (scale bar = 750 μm).

Cohen *et al.* fabricated hydrophilic patterns on superhydrophobic surfaces with water harvesting characteristic similar to the Namib desert beetle.[62] These patterns were prepared by depositing polyelectrolyte spots with different surface free energy to the superhydrophobic surface. The surface free energy of the polyelectrolyte spots can be regulated by changing the specific functional terminal groups distributed over the top patterned surface of a hydrophobic fluorine-containing resin and hydrophilic polyacrylic acid (PAA) (Fig. 4C and D). Badyal *et al.* have mimicked the Stenocara beetle's back for water collection using plasma treated surfaces with patterned superhydrophobic–hydrophilic/superhydrophilic microdomains.[63] Plasma-fluorinated polybutadiene and plasma etched poly(tetrafluoroethylene) were used as the two kinds of superhydrophobic substrates. The chemical nature of the hydrophilic microdomains plays an important role in water collection and superhydrophilic poly(4-vinylpyridine) spots exhibited the greatest efficiency for water capture. The optimum hydrophilic pixel size/center-to-center distance of 500 μm/1000 μm resembles the feature size of the hydrophilic–hydrophobic pattern on a Stenocara beetle's back. Recently, Ruhe *et al.* prepared various polymer based superhydrophobic surfaces with selectively patterned hydrophilic domains and investigated the influence of the wettability, surface geometrical parameters and tilting angles on the critical volume of water droplets which dewetted from the circular defects and rolled off from the subtrates.[64] The result indicated that the pinning force for a given bump was constant and did not depend on the drop volume. These patterned surfaces, mimicking the back of the Stenocara beetle, can collect water if exposed to a foggy atmosphere.

1.4 Self-healing extreme wettability

Self-healing ability is the most remarkable property of a biological system. A repair response occurs in a biological system when the damage site sends out chemical signals, and repair agents are transported to the site of injury to complete self-healing. It is the self-healing character that makes natural examples, *i.e.* plant leaves with superhydrophobic properties, maintain superhydrophobicity during their lifetime. Unlike nature's creatures that can repair or reconstruct surfaces to maintain their surface wettability, manmade superhydrophobicities are mostly very weak to mechanical contact for their ultrafine structures; what's more, they can rarely be repaired automatically, which makes the artificial surfaces lose their "self-cleaning" function in a short time. It is extremely difficult for artificial self-healing system to mimic the perfect self-healing function of natural surfaces. A successive supply of surface coating materials in natural system is another aspect of self-healing. Bhushan *et al.* have studied the surface structures or wax regeneration of small pieces of fresh, water-containing plant specimens by AFM.[65] The regeneration of epicuticular wax films on living plant surfaces is a dynamic and fast process. The process of wax film formation occurs by self-assembly of the wax molecules into layered structures (Fig. 5). Wang *et al.* have studied surface property recovery of a living clover leaf and made comparisons with a dead leaf. Both the living leaf and the dry clover leaf are superhydrophobic initially (Fig. 6A and D).[66] When they were treated with O_2 plasma even for 10 s, they turned superhydrophilic (Fig. 6B and E). Afterwards, the living leaf was raised in soil for recovery and recovered its superhydrophobicity and low adhesion after 48 h, as shown in Fig. 6C, while the dry clover leaf still remained hydrophilic after being stored for 48 h or even longer (Fig. 6F). The surface chemical composition change was measured by XPS. It shows that for the living clover leaves, the C/O ratio of the original leaf surface was 7.14, and it changed to 3.12 after plasma treatment and again increased to 6.67 after 48 h self-healing. This indicates that the damaged leaf surface coating had recovered because of the self-healing capability. However, the C/O ratio of dry leaf surface after plasma treatment dramatically decreased and most importantly could not return to the original level. The evidence verifies that the mother bio-species can endow the natural superhydrophobic surfaces with strong ability to self-heal their superhydrophobicity by consecutively refreshing the surface coating.

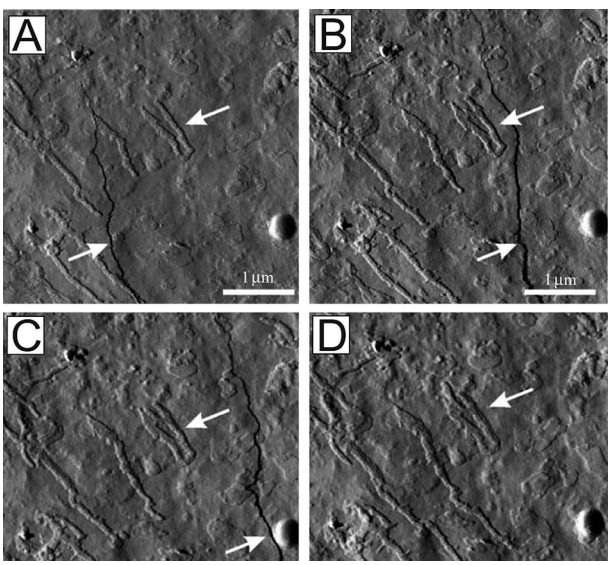

Fig. 5 AFM images of a multilayer wax film formation on *uniflorum*. In (A), recorded 32 min after removal of the original waxes, the formation of the S-layer film is denoted by the upper arrow. The edge of a second, rapidly growing layer is denoted by the lower arrow. In (B), only 4 min later, the wax layer has grown underneath the S-layer structures. In (C), recorded another 4 min later, the wax layer has covered nearly 80% of the scanned area, whereas the S-layers grew very slowly. (D) After a total time of 53 min, the scanned surface area is completely covered with a new wax layer. (Self-healing of voids in the wax coating on plant surfaces.)

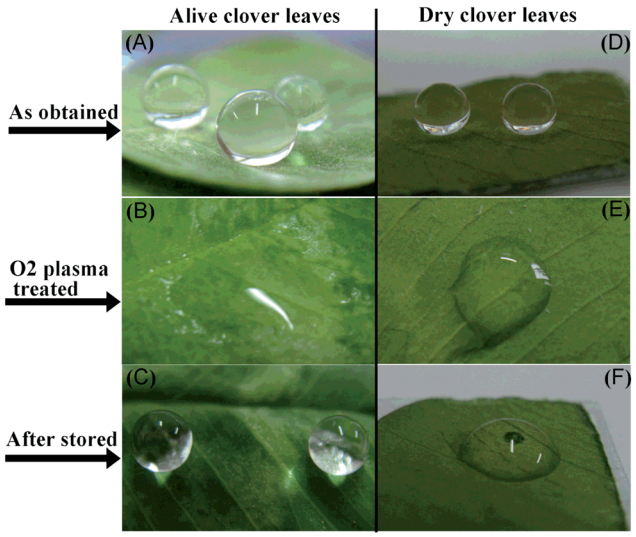

Fig. 6 Photos of water droplets on different clover leaves, (A) alive clover leaf; (B) alive clover leaf after O_2 plasma treatment for 30 s; (C) alive clover leaf with 48 h-healing after plasma treatment; (D) dry clover leaf; (E) dry clover leaf after O_2 plasma treatment for 30 s; (F) dry clover leaf with 48 h-storage after 30 s O_2 plasma treatment.

For real application of surfaces with extreme wettability, people should think more about nature's way. Biomimicking self-healing surfaces will inspire people to research biomimicry from a static to a dynamic, living system. Unfortunately this has been largely omitted in the last ten years. People have started to realize the importance of dynamic maintenance of extreme wettability and a few successful examples will be discussed in the following section.

2 Biomimicking beyond nature?

People have learned very well from nature in recent years. But the most important characteristic of being a human is to do better than nature. In addition, to mimic the special wettability existing in nature, artificial surfaces with exceptional wetting properties have also appeared, and these surface properties cannot be found in nature, such as reversible switchable wettability, reversible switchable water/oil droplet adhesion, superoleophobicity at the air–solid interface or under vacuum and self-healing superamphiphobicity, and thus we just call them "biomimicking beyond nature".

2.1 Reversible switchable wettability

Reversible switchable wettability means that the chemical composition and/or surface topography of a single surface under the external stimuli can be reversibly altered between two different states between (super)hydrophobicity and (super) hydrophilicity. To make surfaces with switchable wettability, materials with different responsive properties have been implemented, primarily on a rough surface with enhanced wettability contrast when they switch their intrinsic properties. Light is one of the most important external stimuli sources.[67–69] Inorganic oxides and organic polymers are two of the most typical photo-responsive materials. Under light illumination, photo-responsive materials can often reversibly change their electronic structure and molecular geometric/conformation in solutions, crystals, and gels; these changes then induce physical property changes such as those of polarity, fluorescence, refractive index, and magnetism *etc*. Among the photo-sensitive inorganic oxides, TiO_2 is the most studied semiconductor. When the surface of TiO_2 is irradiated by UV light, the photo-generated cavity will react with the lattice oxygen to form surface oxygen vacancies that can combine with water molecules to form hydroxyl group. The hydroxyl group can greatly increase the surface energy, and the hydrophilicity was enhanced under the action of hydrogen bonding. Fujishima *et al.* reported that the water CA of anatase TiO_2 polycrystalline films can switch between 72° and 0° with the alternated irradiation of UV and Vis.[70–72] Subsequently, switchable wettability was amplified on structural TiO_2 surfaces between superhydrophobicity (CA > 150°) and superhydrophilicity (CA ~ 0°) (Fig. 7A).[73] In addition to TiO_2, films made from some other photoresponsive semiconductor inorganic oxides also possess switchable wettability properties such as ZnO,[74,75] WO_3,[76] V_2O_5[77] and SnO_2[78] *etc.*, *via* a very similar mechanism. Moreover, some photo-responsive organic materials can also be used for switching surface wetting due to a reversible molecular conformation change. These molecules include azobenzenes,[79] spiropyrans,[80] dipyridylethylenes,[81] stilbenes[82] and pyrimidines[83] *etc*. Among them, azobenzene and its derivatives are the most widely used materials[84] that under visible light present the *trans*-conformation having a small dipole moment and a low surface free energy and after exposure to UV turn to the *cis*-conformation having a large dipole moment and so a little higher surface free energy.[85] By introducing low free energy groups such as $-CF_3$ groups into the terminal functional groups on the side chain of azobenzene molecules and surface structuring, superhydrophobic/superhydrophilic transition can be achieved (Fig. 7B).[86]

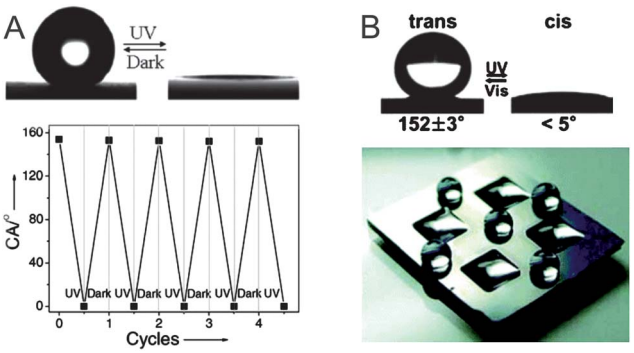

Fig. 7 (A) Photographs of a spherical water droplet switch between superhdyrophobicity (CA ~ 154°) and superhydrophilicity (CA ~ 0°) before and after the UV illumination and corresponding switch cycles on rough TiO_2 surface. (B) Superhydrophobic/superhydrophilic transition of fluorine contained AZO molecules on rough $(PAH/SiO_2)_9$ multilayer film and corresponding selective UV irradiation of patterned rough substrate.

Temperature can change the way materials interact with surroundings and their affinity to the environment, therefore it can easily regulate the surface free energy and wettability. Poly(*N*-isopropylacryl-amide) (PNIPAAm) is a well-known temperature-sensitive polymer with a lower critical solution temperature (LCST) of about 32 °C.[87–90] Below the LCST, the intermolecular H-bonding between PNIPAAm chains and water molecules is predominant, which results in swelling of polymer chains and hydrophilicity. Above the LCST, intramolecular H-bonding among the PNIPAAm chains results in collapsed chain conformation and so the hydrophobicity (Fig. 8A).[91,92] Based on this kind of temperature sensitive property, reversible switching wettability can be easily realized by regulating environmental temperature below or above LCST. Sparsely grafted PNIPAAm brushes on anodized alumina surfaces with hydrophobic background don't significantly change the surface wetting properties, but lead considerably to surfaces with responsive wetting transitions and hysteresis characteristics. When the probing droplet interacts with polymers and they become hydrated, the wetting can be easily realized from the Cassie mode to the Wenzel mode, with the characteristics of high hysteresis and a decrease in contact angle after external pressure applied. On the other hand, if the probing droplet doesn't interact with polymers, meaning that polymer will remain in a collapsed state, the droplet will remain in the stable Cassie wetting mode even if external pressure is applied (Fig. 8B).[93] In addition to PNIPAAm, some other thermo-responsive polymers that possess temperature responsive properties are also summarized in Table 1.

Weak polyacids and weak polybases are two types of pH responsive polymers (Table 1) and have been used to switch surface wetting properties. They transform into polyelectrolytes at high pH (polyacids) or low pH (polybases) with electrostatic repulsion forces between the molecular chains and into neutral polymer at low pH(polyacids) or at high pH (polybases). This gives a momentum along with the hydrophobic interaction to govern precipitation/solubilization of molecular chains, deswelling/swelling of hydrogels, or hydrophobic/hydrophilic characteristics of surfaces.[94] Jiang *et al.* reported that poly(styrene-methyl methacrylate-acrylic acid) crystal films in the presence of sodium dodecylbenzenesulfonate (SDBS) could show pH-responsive properties.[95] At low pH (pH = 6) the carboxyl group existed in the form –COOH which would form hydrogen bonding with SO_3^- of SDBS, and thus the hydrophobic long alkyl chain would be exposed outside leading to superhydrophobic states (CA ~ 150.4 ± 0.8°). After treatment with base solution (pH = 12), deprotonation of –COOH to $-COO^-$ make the PMAA swollen state. Hydrophilic groups of $-COO^-$ and $-SO_3Na$ were both exposed to the surface resulting in superhydrophilicity (CA ~ 0°)(Fig. 9 A–D). Liu *et al.* reported that

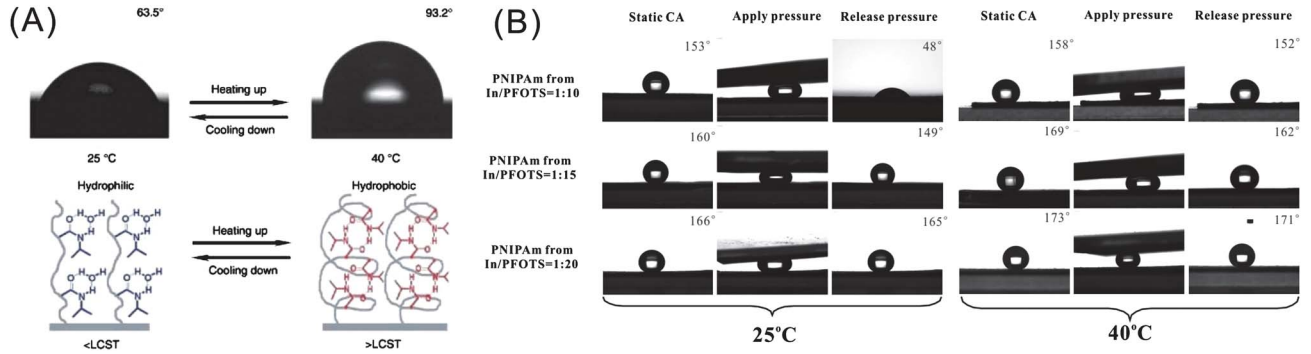

Fig. 8 (A) Thermally responsive wettability for a flat PNIPAAm-modified surface and diagram of reversible formation of intermolecular hydrogen bonding between PNIPAAm chains and water molecules (left) and intramolecular hydrogen bonding between C≡O and N–H groups in PNIPAAm chains (right) below and above the LCST. (B) Optical images of wettability changes of PNIPAm (from different ratios of In/PFOTS) grafted anodized alumina substrates under external pressure at 25 °C and 40 °C, respectively.

a polydimethyaminomethacrylate (polybase) grafted anodized alumina shows switchable wettability between superhydrophobicity and hydrophilicity based on the deprotonation and protonation of the amine groups (Fig. 9E, F).[92] Furthermore, some polycations (polyelectrolytes state of the polyacids or polybases)[96,97] and some ionic liquids[98,99] could also realize switchable wettability by counterion exchange.

Treated by different solvents, heterogeneous (mixed) polymer brushes (HPBs)[100] and some segmented copolymer[101–103] would show different chain conformation because of the different solubility of different components and blocks, and this phenomenon will further influence the surface free energy which offers a possible way to realize switchable wettability. Minko *et al.* fabricated two-level structured self-adaptive surfaces.[100]

Table 1 Summary of usual stimuli-responsive organic and inorganic materials

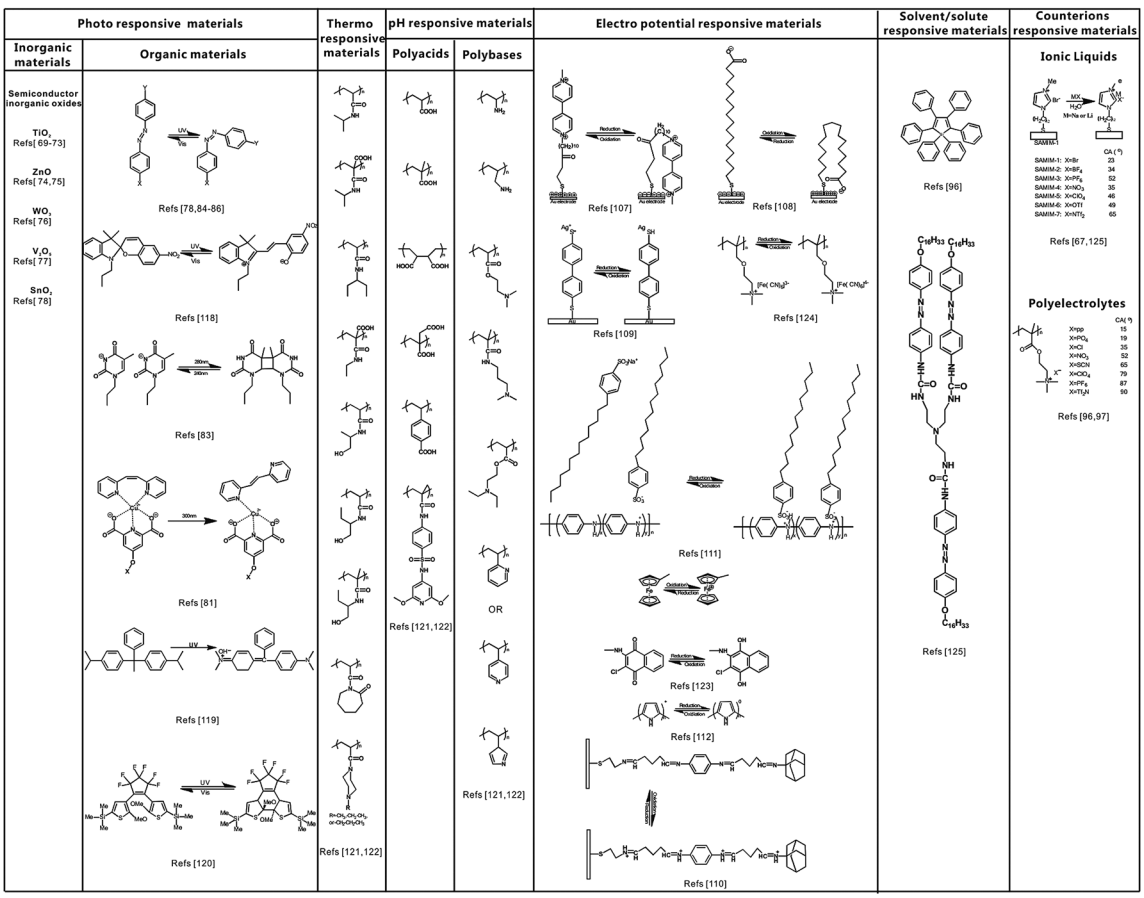

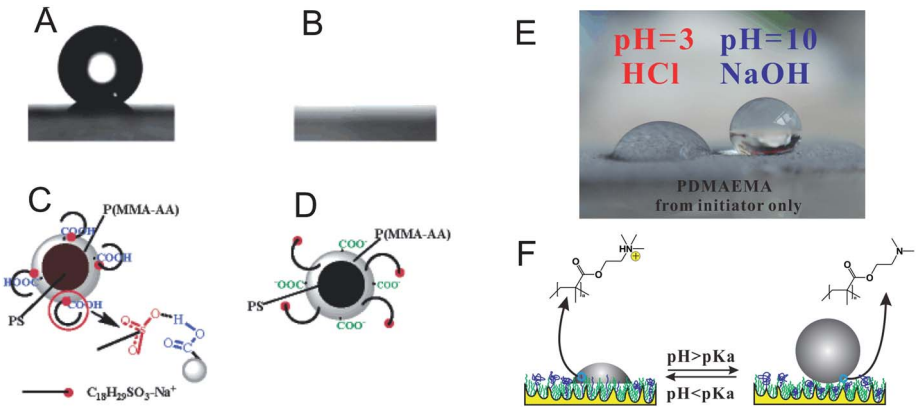

Fig. 9 (A, B) Photographs of water droplet shape on the films assembled from suspensions with pH of 6.0 and 12, respectively; (C, D) illustrations of the structure of the latex sphere in the films of parts A and B, respectively. (The conformation of hydrogen bonding is noted by the arrow.) (E) Digital images of pH = 3 and pH = 10 droplet shape on PDMAEMA only modified anodized alumina surface, and (F) corresponding schematic illustration.

The first level of structure is built by a rough polymer film that consists of needlelike structures of micrometre size. The second level of structure is formed by the nanoscopic self-assembled domains of a demixed polymer brush irreversibly grafted onto the needles. By exposing the surface to solvents that are selective to one of the components of the brush, they reversibly tune the surface properties. The large scale surface structure amplifies the response and enables them to realize switchable wettability between superhydrophobicity and superhydropohicity.

Recently, Sun *et al.* reported a chirality-triggered wettability switching on a smart three component copolymer surface, and the copolymer was composed of three functional units: chiral recognition unit, mediating unit and functional switching unit.[104] They demonstrated that the CAs of a copolymer modified textured silicon substrate after treatment with the D-lyxose solution with different concentrations can switch between superhydrophobicity (CA $\sim$ 157 $\pm$ 2°) and hydrophilicity (CA $\sim$ 42 $\pm$ 2°) for the responsiveness of the chiral recognition unit. On the contrary, the chiral recognition unit almost doesn't respond to L-lyxose. The large extent of reversible wettability switching and the differential volume change of the film induced by the *enantio*-selective binding and release toward monosaccharide enantiomers are expected to be used in chiral separation, chiral medicine, smart microfluidic devices, and bio-devices,[105] *etc.*

Electrical potential (EP) can also be used as an external stimulus for its fast response to control the surface chemistry and/or morphology. Therefore, organic molecules with EP-responsive properties could be used to fabricate or design surfaces with switchable wettability properties (Table 1).[106,107] By regulating the external EP, EP-responsive materials can be switched between reduction state and oxidation state, bringing about the possibility of switch between hydro(oleo)phobicity and hydro(oleo)philicity.[108–111] As an example, Xu *et al.* have fabricated superhydrophobic polypyrrole (PPy) films[112] that turned superhydrophilic after oxidation (Fig. 10). Wettability can be changed by alternating the external electrical field.[113–117] In this case no redox reaction occurs, but a change in charge density across the solid–liquid interface happens, which decreases the solid–liquid interfacial tension.

2.2 Droplet mobility control

Surfaces that can reversibly alter droplet mobility have not been found in nature. These surfaces are more useful in practice than those only having the sticky or pinning effect on droplets. Tunable control of droplet mobility can also be realized by regulating surface chemical composition and/or surface morphology. Liu *et al.* reported that water droplets can be pinned on superhydrophobic PDMS/PTFE replicas with randomly distributed hydrophilic molecules (PSSNa), and water droplet can freely roll on the replicas after these hydrophilic molecules are washed away.[54] Lin *et al.* reported a simple electrochemical and self-assembly method for fabricating superhydrophobic spongelike nanostructured TiO_2 surfaces with markedly controllable adhesion. Water adhesion ranging from ultralow (5.0 μN) to very high (76.6 μN) can be tuned through adjusting the nitro cellulose dosage concentrations.[59] Afterwards they fabricated porous TiO_2 surfaces with different pore sizes. By modifying the porous TiO_2 surfaces with 1*H*,1*H*,2*H*,2*H*-perfluorooctyltriethoxysilane, the adhesion force to water droplets can be tuned in a wide range.[60]

However, the above-mentioned surfaces of this section with tunable adhesion properties are all conducted on different samples. One would expect switching the adhesion on a single

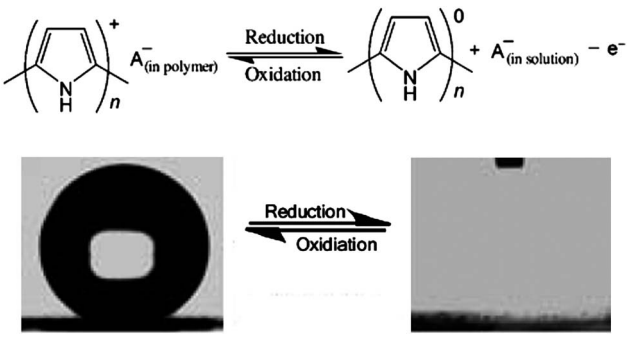

Fig. 10 Schematic illustration of the reduction and oxidation state of PPy and corresponding superhydrophobic/superhydrophilic switch of water droplet.

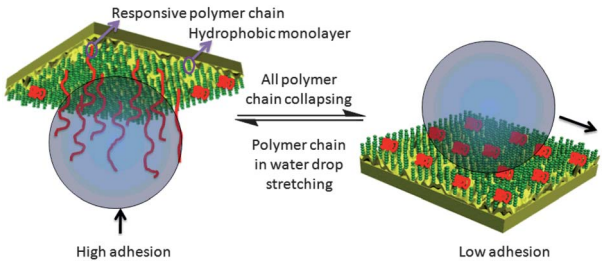

Fig. 11 Schematic illustration of the general mechanism on reversible adhesion of water droplets induced by macromolecular anchors on hydrophobic molecule-modified Al_2O_3 substrate.

surface. A versatile mechanism for designing such surfaces is demonstrated in Fig. 11, in which dilute responsive polymer chains are grafted onto hydrophobic backgrounds and their response to external stimuli in liquid droplet determines the surface adhesion.[92] Jiang *et al.* reported that they realized reversible switching of water droplet mobility from a rollable state to pinned state on a superhydrophobic surface with optimized roughness.[126] The precise coordination of the roughness and the interfacial chemistry response are essential to obtain the droplet mobility switching (Fig. 12). Liu *et al.* have demonstrated a general method to reversibly switch the mobility of droplets on rough surfaces containing dilute responsive polymer chains.[92] The surfaces are nonwettable, and droplets roll off surfaces when the polymer chains are in the collapsed state and have weak interaction with droplet when the environmental temperature is higher than the LCST of PNIPAm, the pH of the probing droplet is higher than the pK_a of PDMAEMA, or probing droplets containing hydrophobic counterions. However, when the polymers interact strongly with the droplets, they can restrict their movement on the surface. The switching behavior is fully

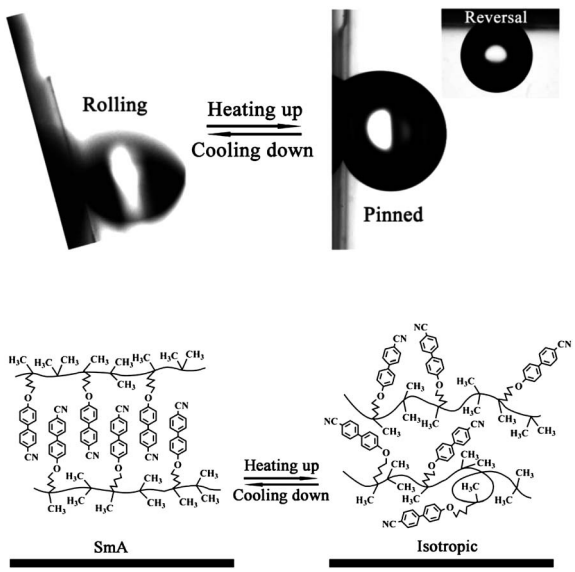

Fig. 12 The reversible switching of water droplet mobility from rollable to pinned corresponding to the temperature change from 23 °C (left, SA = 75 ± 3°) to 75 °C (right, the inset shows that the droplet sticks on the surface even when the substrate is turned upside down) and the proposed conformation rearrangement upon the phase transition.

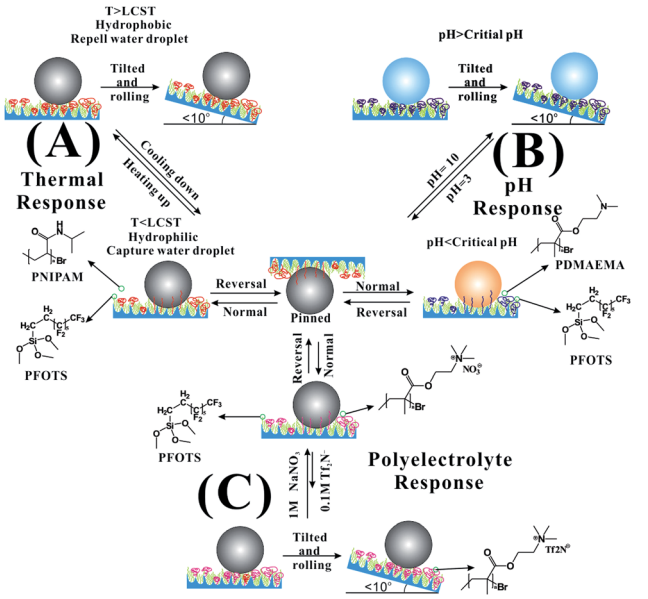

Fig. 13 Schematic illustration of (A) thermo-responsive (PNIPAm) surfaces, (B) pH responsive (PDMEMA) surfaces and (C) polyelectrolytes responsive (Q-PDMAEMA) surfaces with properties of switching water droplet adhesion.

reversible and can be extended to other responsive polymer systems. These surfaces will find applications in microdroplets in microfluidics, smart coatings, and self-cleaning surfaces (Fig. 13). The surface adhesion can also be switched in response to light irradiation. A superhydrophobic TiO_2 nanotube surface was selectively illuminated with UV through a mask to create alternatively arranged hydrophilic/superhydrophobic regions.[127] The separately distributed hydrophilic regions increase water adhesion, while the surrounding superhydrophobic areas prevent the spread of water droplets and preserve superhydrophobicity (Fig. 14A). The recovery was very fast upon heating at a relatively high temperature. Similarly, water droplet mobility can be reversibly manipulated by using a photo-responsive coating on a rough surface. The surface coating consists of a structural silicone elastomer as the basic hydrophobic material and the incorporated low concentration azobenzene compound as the molecular photosensitizer that assumes *trans–cis* conformation change under Vis and UV illumination. The surface thus could switch between low SA and high SA states when azo-compound assumes *trans*- and *cis*-conformations, while the surface superhydrophobicity doesn't change apparently (Fig. 14B).[85] Sun *et al.* have demonstrated that the adhesion force and the sliding angles show strong dependence on the surface curvature on a PDMS surface with a regular array of pillars, giving the possibility of reversibly switching droplet adhesion between pinned and roll-down superhydrophobic states.[128] The responsive surface has potential applications in controlling droplet mobility in microfluidic devices.[129]

2.3 Superoleophobicity

Self-cleaning surfaces with superhydrophobicity can be easily found in nature. However, superoleophobic surfaces in air that possess super repellent properties to oils with much lower surface

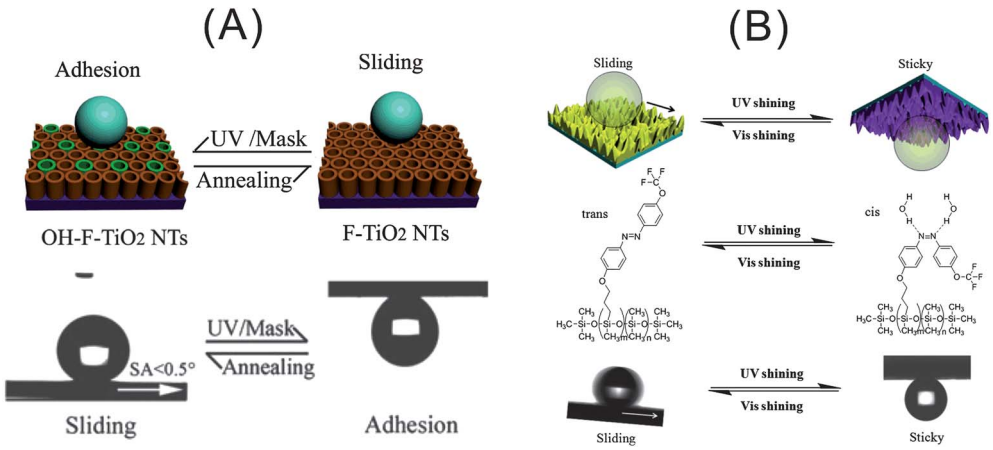

Fig. 14 Schematic illustration of the mechanism of (A) producing TiO_2 nanotubes with switchable wettability and adhesion and the corresponding digital images and (B) water droplet reversible adhesion on PDMS and azobenzene modified anodized alumina upon UV and vis irradiation and corresponding digital images.

tension are rare, probably because very few biological creatures live in an oily environment. Recently Liu *et al.* prepared a surface structure by mimicking the surface of fish skin. The artificial surface possesses low-adhesive superoleophobic properties, but only at the oil–water–solid three-phase interface (Fig. 15 A–C). It shows superoleophilicity in air (biomimicking from nature).[130] Artificial superoleophobicity in air is also an important special wettability beyond nature. The superoleophobic surface has wide application potential for the prevention of oil contamination in many cases. Fabrication of superoleophobic surfaces can follow the same design principle as that of artificial self-cleaning surfaces, but are rarely successful.[131,132] This largely comes from the similarly low surface tension of oils to the commonly used low energy coating materials, mainly the perfluoro-compounds and silicones. To achieve such a surface would require the coating material to have a surface tension value lower than 6 mN m^{-1}, which is absent in reality (the $-CF_3$ group has a theoretical surface energy of 6 mN m^{-1}). Tsujii *et al.* reported a super oil repellent surface of rough anodized alumina that after the modification by fluorinated monoalkylphosphates is super repellent to rapeseed oil (γ_{lv} = 35.0 mN m^{-1}) with a CA of 150°, and is oleophobic to decane (γ_{lv} = 23.8 mN m^{-1}) with a CA about 120°.[133] Thus the lower the surface tension of oil droplets, the harder the superoleophobicity can be realized. The concept of

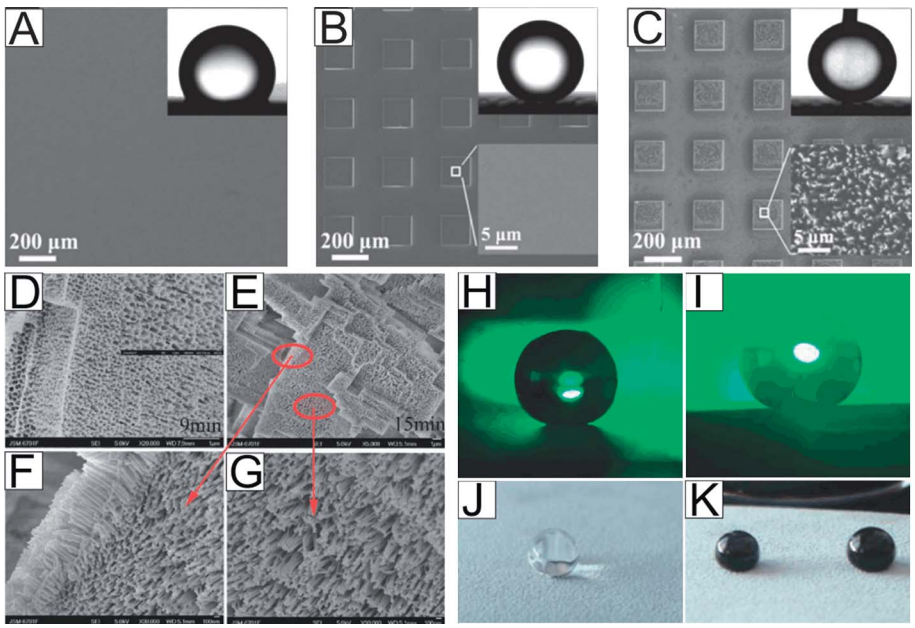

Fig. 15 Photographs of oil droplets on different surfaces in water (A) smooth silicon surface, (B) microstructured silicon surface, (C) micro/nano-structured silicon surface. SEM images of high field anodic oxidation for different time periods (D) 9 min, (E) 15 min, (F) and (G), are the corresponding high magnifications. Photos of representative liquid droplets (H) water, (I) hexadecane, (J) silicone oil, (K) crude oil on the super oil repellent anodized alumina surfaces in air.

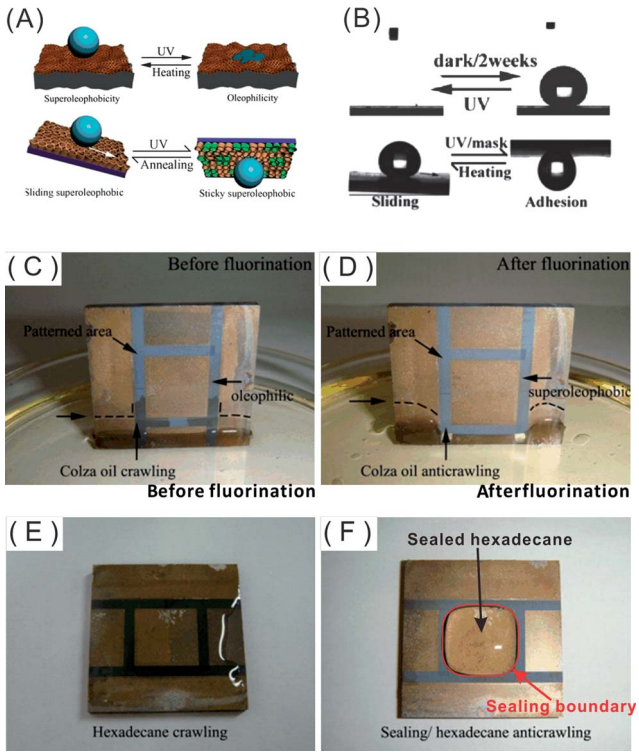

Fig. 16 (A) The schematic illustration of mechanism of patterned TiO_2 surfaces with switchable wettability and adhesion to oil droplets and (B) the corresponding digital images. (C, E) Oil drop crawling and wetting on control surface; (D, F) anticrawling and sealing with superoleophobic surfaces.

combining the fractal surface dimension and the compact packing of trifluoromethyl groups on it has been verified to be a valid guiding principle. Cohen *et al.* have reported two different approaches (electrospinning and ion etching) to fabricate surfaces possessing re-entrant curvature.[134] After modification with low surface energy materials such as fluorooctyl polyhedral oligomeric silsesquioxane (POSS) or 1*H*,1*H*,2*H*,2H-perfluorodecyltrichlorosilane, the surface possessed super oil repellent properties to decane (γ_{lv} = 23.8 mN m^{-1}) and/or octane (γ_{lv} = 21.6 mN m^{-1}). The re-entrant curvature as a third factor besides the roughened texture and low surface energy materials plays the most important role in the design of extremely robust nonwetting surfaces.

Wu *et al.* have demonstrated an easy and industry compatible approach to achieve super-repellency to a broad range of liquids at the air–solid interface.[41] These surfaces are fabricated by forming an alumina forest *via* simple electrochemical method and post modification with hydrophobic materials (Fig. 15D–G). Upon modification with perfluorosilane, the surface turns super-repellent to a broad range of liquids, which includes (salted) water (γ_{lv} = 72.0 mN m^{-1}), water emulsion, common organic liquids, like glycerol (γ_{lv} = 50.0 mN m^{-1}) and alkanes (hexadecane, γ_{lv} = 27.6 mN m^{-1}), and a variety of lubrication oils inclusive of ionic liquids, crude oil, poly(α-olefin) (γ_{lv} = 27.0 mN m^{-1}), and even silicone oils (γ_{lv} = 22.0 mN m^{-1}) *etc.* (Fig. 15H–K). The surfaces have potential applications in preventing lubrication oil creep, anti-oil contamination and de-waxing in oil pipeline transportation *etc*. Steele *et al.* have created a superoleophobic nanocomposite coating that can be easily applied by spray casting waterborne perfluoroacrylic polymer emulsion containing ZnO nanoparticle.[135] Cohen *et al.* have developed a simple and environment benign dip-coating process that enables them to provide a flexible and conformal coating of extremely low-surface-energy fluorodecyl POSS molecules on any surface. The synergistic effect of roughness, re-entrant topography of the substrate, and the low surface energy of fluoro-POSS molecules enables the surfaces to support even very-low-surface-tension liquids. By combining this understanding, on a conformal and flexible fluorinated coating, they reversibly switched the wetting behavior of fabric surfaces between super-wetting and super-repellent with a wide range of polar and nonpolar liquids using simple mechanical deformation.[136] Wang *et al.* realized the reversible switching on the wettability of oil droplets (between superoleophobicity and superoleophilicity) and reversible adhesion of oil droplets (between sliding superoleophobicity and sticky superoleophobicity) on TiO_2 surfaces through alternating treatment by UV and annealing (Fig. 16A and B).[137] Other proof-of-concept applications of the surface are shown in Fig. 16C–F, where the grey area was patterned and anodized. The substrate was standing with the bottom being immersed into colza oil. Without perfluorination, the surface is oleophilic, colza oil climbs up, much faster along a patterned area that is more oleophilic (Fig. 16C).

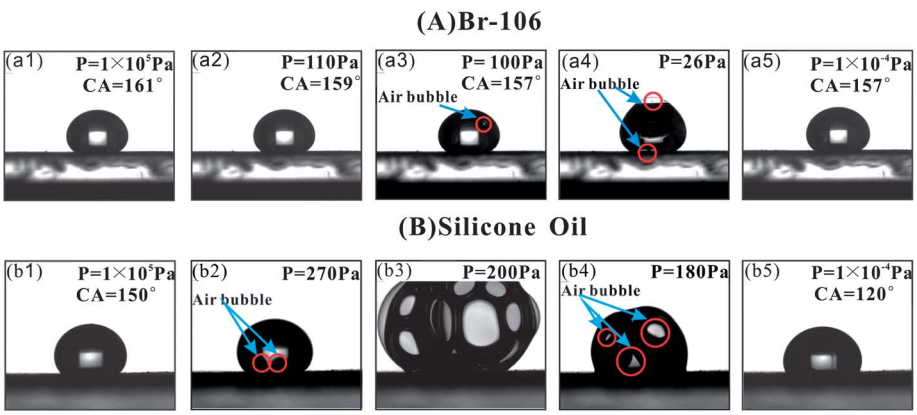

Fig. 17 Images of the change in contact angles of (A) Br-106 and (B) silicone oil during vacuum-pumping.

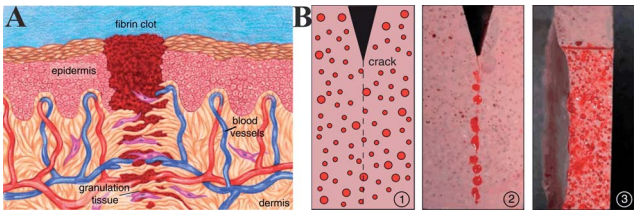

Fig. 18 (A) Schematic of an intermediate stage of biological wound healing in skin. Tissue damage triggers bleeding, which is followed by the formation of a fibrin clot. Fibroblast cells migrate to the wound site enabling the creation of granulation tissue to fill the wound. (B) Demonstration of bioinspired damage-triggered release of a micro encapsulated healing agent in a polymer specimen: (1) schematic of compartmentalized healing agent stored in a matrix; (2) release of dyed healing agent into the crack plane, which leads to a synthetic clotting (polymerization) process to bond the crack faces; and (3) one-half of the fracture surface revealing ruptured capsules.

After fluorination, the substrate turns oleophobic, especially superoleophobic in patterned areas. It is seen from Fig. 16D that oil climbs much faster along a less oleophobic unpatterned area, while being obstructed by a patterned superoleophobic area. When a hexadecane drop is dropped onto the oleophilic surface (without perfluorination), it spreads very quickly and wets the whole surface (Fig. 16E). However, a drop of hexadecane stays within a patterned framework and further spreading is stopped (Fig. 16F). The configuration can be used for sealing and storage of oil samples, especially when oil leakage can cause serious problems. Seeger *et al.* reported a simple grow-from approach for the fabrication of superoleophobic surfaces by the combination of versatile organosilanes.[138] They demonstrated that the topography of the nanofilament layer plays an important role in influencing superoleophobicity of the surfaces and can be regulated simply by the water concentration in toluene during the TCMS (trichloromethylsilane) coating procedure, and furthermore the superoleophobic coatings show very good transparency and chemical and environmental durability.

Superoleophobicity allows the study of extreme wetting under vacuum because of the low volatility of many synthetic oils. According to the Cassie wetting model, droplets sit on a solid–air composite surface of which the air fraction can be above 90%. However, the vacuum wettability study verifies that superoleophobicity for certain liquids does exist even without vapour phase (Fig. 17A), in which the droplet remains suspended entirely through the action of the surface tension of the drop above a composite vacuum-solid rather than air–solid surface. The wetting mode is termed the "vacuum-Cassie–Baxter" state (Br-106, ionic liquids based on 1-methyl-3-hexyl imidazolium bromine, $\gamma_{lv} = 38.0$ mN m^{-1}). However, for other liquids of even lower surface tension (silicone oil, $\gamma_{lv} = 22.0$ mN m^{-1}), the same surface doesn't exhibit superoloephobicity (Fig. 17B).[139]

2.4 Artificial self-healing (super)amphiphobic surfaces

So far, the artificial surfaces created are mostly "static" surfaces, while the surfaces that can "dynamically" preserve extreme wettability are highly desired for their practical applications, for which the self-healing function is expected. Both the surface morphology and the surface composition can be damaged during service, which however, can be perfectly recovered in nature. To restructure surface morphology is not as easy as to recover surface composition. Self-healing materials are inspired by living systems in which minor damage (*e.g.* a contusion or bruise) triggers an autonomic healing response.[140] Successful healing relies on seamless integration of reactive chemical functionality into polymer or polymer composite at the microscale, nanoscale, or molecular level.[141–143] Many fractured or critically damaged living tissues can heal themselves by the formation of an intermediate tissue (based on the response to inflammation) followed by the scar tissue.[144] The biological processes control tissue

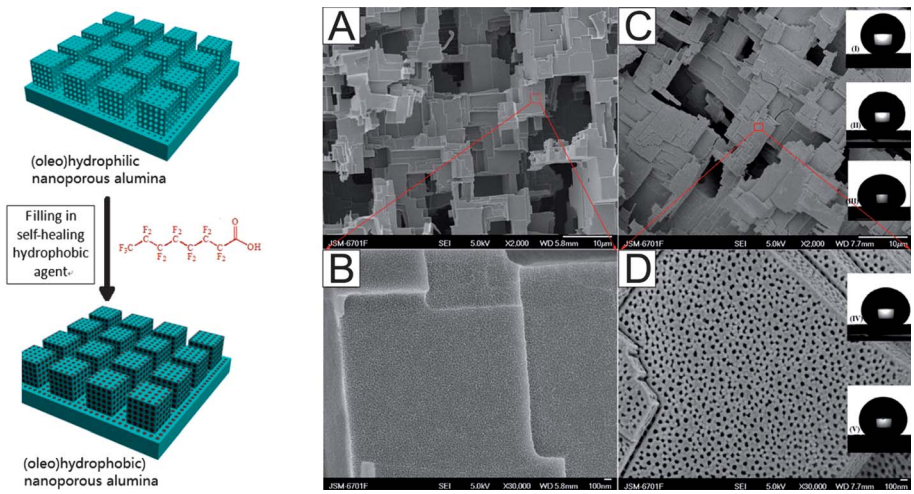

Fig. 19 Left: schematic depiction of wettability changes of a nanoporous alumina substrate and filling in hydrophobic perfluorooctyl acid. The (oleo) hydrophobic surfaces possess self-healing capability due to gradual release of perfluorooctyl acid. Bottom: SEM images of anodized alumina without nanopores (A, B), and with high density nanopores (C, D, proportion of pores is about 60%, mean pore diameter is 40 nm and mean depth is 300 μm). The insets are snapshots of representative liquid droplets on the perfluorooctyl acid loaded nanoporous alumina: (I) water, (II) glycerol, (III) CH_2I_2, (IV) hexadecane, (V) rapeseed oil.

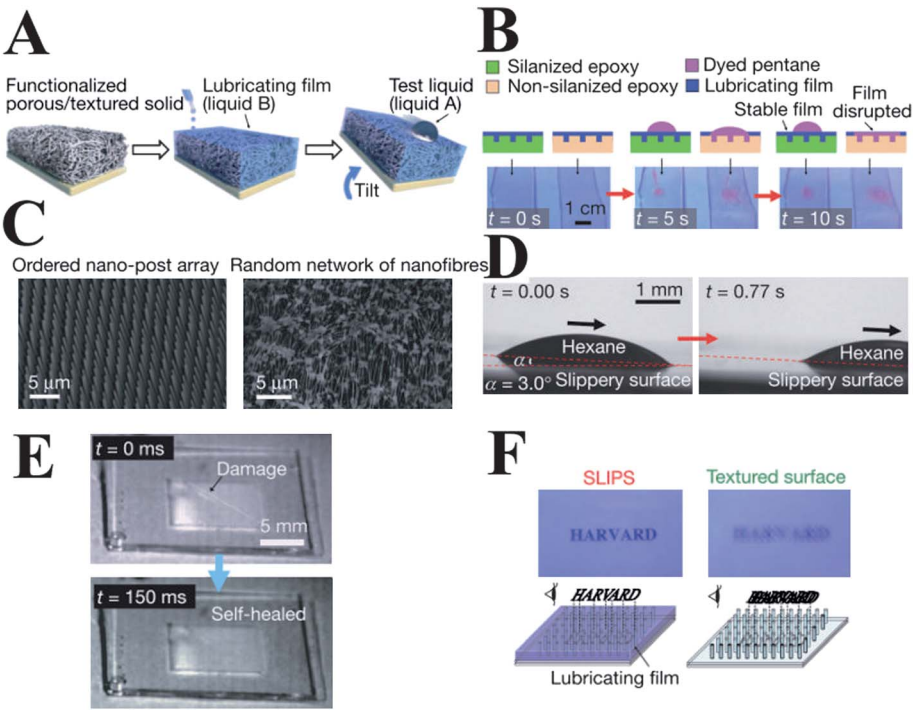

Fig. 20 Design of SLIPS. (A) Schematic showing the fabrication of a SLIPS by infiltrating a functionalized porous/textured solid with a low-surface-energy, chemically inert liquid to form a physically smooth and chemically homogeneous lubricating film on the surface of the substrate. (B) Comparison of the stability and displacement of lubricating films on silanized and non-silanized textured epoxy substrates. (C) Scanning electron micrographs showing the morphologies of porous/textured substrate materials: an epoxy-resin-based nanofabricated post array (left) and a Teflon-based porous nanofibre network (right). (D) Optical micrographs demonstrating the mobility of a low-surface-tension liquid hydrocarbon—hexane ($\gamma_A = 18.6 \pm 0.5$ mN m^{-1}, volume ~3.6 μL)—sliding on a SLIPS at a low angle ($\alpha = 3.0°$). (E) Time-lapse images showing the capability of a SLIPS to self-heal from physical damage, 50 mm wide on a timescale of the order of 100 ms. (F) Optical images showing enhanced optical transparency of an epoxy-resin-based SLIPS (left) as compared to significant scattering in the non-infused superhydrophobic nanostructured surface (right) in the visible light range.

response to injury and repair involves inflammation, wound closure and matrix remodeling.[142] After approximately 24 h, the cell proliferation and matrix deposition begin to close the wound (Fig. 18A). During the final stage of healing (which can take several days), the extracellular matrix is synthesized and remodelled as the tissue regains strength and function (Fig. 18B). However, artificial self-healing wettability has been rarely reported. Design of self-healing surface wettability can borrow ideas from these systems. Ideally, synthetic reproduction of the healing process in a material requires an initial rapid response to mitigate further damage, efficient transport of reactive materials to the damage site and structural regeneration to recover full performance.[145]

Sun *et al.* reported that self-healing superhydrophobic layer-by-layer coatings could be fabricated by preserving healing agents consisting of reacted fluoroalkylsilane in the coatings, which are porous and rigidly flexible.[146] After speeded-up damage of surface hydrophobicity by oxygen plasma, the preserved reacted fluoroalkylsilane can easily migrate to the coating surface especially under a humid ambient environment, resulting in the healing of the superhydrophobicity of the coatings. The self-healing of the superhydrophobic coatings can be repeated several times without decreasing the superhydrophobicity. Plant leaves preserve superhydrophobicity very well and can be recovered or refreshed after damage. However, the plant leaves can only regain their superhydrophobicity but not superoleophobicity. Wang *et al.* have demonstrated a robust anodized alumina surface with self-healing superamphiphobic properties. The surface consists of a large number of nano-pores which are used as nanoreservoirs for low surface energy materials, perfluorooctyl acid.[66] The surface property can be healed by the transportation/enrichment of low surface energy materials trapped in the nanoreservoirs to the outmost surface, which is thermo-dynamically driven by minimizing the surface tension, and its healing capacity should certainly depend on the capacity of the nanoreservoirs in the system (Fig. 19). After the surface was damaged with O_2 plasma, perfluorooctyl acid can migrate and chemically assemble onto surface. The damaged surface can automatically heal its superamphiphobicity, which means surfaces posses both superhydrophobic and superlipophobic properties (oil contact angles bigger than 150°),[147] in 48 h at room temperature and the process can be speeded up by enhanced temperature. The approach is distinctive in its use of simple ingredients, ease of application, mild conditions of self-healing superamphiphobicity and applicability to many types of materials with nanopores or microvascular networks.[148,149] Not only superhydrophobicity (existing in nature) but also superoleophobictiy (not existing in nature) could be realized in the way.

Inspired by the special repellency property of the Nepenthes pitcher plant,[150] Wong *et al.* recently reported "slippery liquid-infused porous surface(s)" (SLIPS) which possess micro/nano-porous structures filled by perfluorinated lubricating liquid

(repairing liquid), resembling the above mentioned two examples.[151] The SLIPS creates a smooth, stable interface that nearly eliminates pinning of the liquid contact line for both high- and low-surface-tension liquids (immiscible liquids with surface tension ranging from $\sim 17.2 \pm 0.5$ mN m^{-1} (n-pentane) to 72.4 ± 0.1 mN m^{-1} (water)), and minimizes pressure-induced impalement into the porous structures. The synthetic surfaces show excellent wetting properties (negligible contact angle hysteresis and low sliding angles) to low surface tension liquids and their complex mixtures (beyond nature), instantaneous and repeatable self-healing, extreme pressure stability and optical transparency (Fig. 20 A–E). They demonstrated that this kind of surface is commercially available and can be used in biomedical fluid handling, fuel transport, anti-fouling, anti-icing, self-cleaning windows and optical devices, and many more areas that are beyond the reach of current technologies. It is anticipated that the introduction of a self-healing function into robust superamphiphobic coatings will open a new avenue to extending the lifespan of superhydrophobic coatings for practical applications.

3 Summary and outlook

In this review, we have briefly presented some recent research development of extreme wettability, such as superhydrophobicity with self-cleaning property inspired by the lotus leaf, superhydrophobic surfaces with high water droplet adhesion inspired by rose petals, superhydrophobic surfaces with water collection property inspired by a desert beetle's back and superhydrophobic surfaces with self-healing properties inspired by plant leaves. These are the successful examples of biomimicking from nature to artificial. The main focus of this review is the special wetting behavior of artificial surfaces which cannot be found in nature, and thus we call them "biomimicking beyond nature". These special wetting behaviors are mainly embodied in four aspects, reversible switchable wettability between (super) hydrophobicity and (super)hydrophilicity, reversible switchable water/oil droplet adhesion between superhydrophobic pinning states and superhydrophobic rolling state, superoleophobicity at the air–solid interface or even under vacuum, and self-healing (super)amphiphobicity at the air–solid interface. People will continue to work on design and fabrication of surfaces with much faster and smarter responsive property and realize the reality of *in situ* switching of wetting and adhesion. The new progress towards self-healing design will afford surfaces with mechanical robustness, abrasion and contamination resistant and durability *etc.*, and thus surfaces with self-repairable characters would be a promising research direction in the area for the sake of the real applications in micro-fluidics, micro-reactors, oil transportation and automotive and aerospace devices.

Acknowledgements

NSFC(21125316 and 50835009).

References

1 R. Blossey, *Nat. Mater.*, 2003, **2**, 301.
2 Z. G. Guo and W. M. Liu, *Plant Sci.*, 2007, **172**, 1103.
3 W. Barthlott and C. Neinhuis, *Planta*, 1997, **202**, 1.
4 C. Neinhuis and W. Barthlott, *Ann. Bot.*, 1997, **79**, 667.
5 E. Bormashenko, Y. Bormashenko, T. Stein and G. Whyman, *J. Colloid Interface Sci.*, 2007, **311**, 212.
6 X. F. Gao and L. Jiang, *Nature*, 2004, **432**, 36.
7 A. R. Parker and C. R. Lawrence, *Nature*, 2001, **414**, 33.
8 Y. M. Zheng, X. F. Gao and L. Jiang, *Soft Matter*, 2007, **3**, 178.
9 Y. M. Zheng, H. Bai, Z. B. Huang, X. L. Tian, F. Q. Nie, Y. Zhao, J. Zhai and L. Jiang, *Nature*, 2010, **463**, 640.
10 T. Onda, S. Shibuichi, N. Satoh and K. Tsujii, *Langmuir*, 1996, **12**, 2125.
11 W. Chen, A. Y. Fadeev, M. C. Hsieh, D. Oner, J. Youngblood and T. J. McCarthy, *Langmuir*, 1999, **15**, 3395.
12 M. Callies and D. Quere, *Soft Matter*, 2005, **1**, 55.
13 T. L. Sun, L. Feng, X. F. Gao and L. Jiang, *Acc. Chem. Res.*, 2005, **38**, 644.
14 D. Quere, *Annu. Rev. Mater. Res.*, 2008, **38**, 71.
15 P. Roach, N. J. Shirtcliffe and M. I. Newton, *Soft Matter*, 2008, **4**, 224.
16 X. M. Li, D. Reinhoudt and M. Crego-Calama, *Chem. Soc. Rev.*, 2007, **36**, 1350.
17 N. J. Shirtcliffe, G. McHale and M. I. Newton, *J. Polym. Sci., Part B: Polym. Phys.*, 2011, **49**, 1203.
18 Z. G. Guo, W. M. Liu and B. L. Su, *J. Colloid Interface Sci.*, 2011, **353**, 335.
19 A. B. D. Cassie and S. Baxter, *Trans. Faraday Soc.*, 1944, **40**, 0546.
20 A. Lafuma and D. Quere, *Nat. Mater.*, 2003, **2**, 457.
21 T. Wagner, C. Neinhuis and W. Barthlott, *Acta Zool.*, 1996, **77**, 213.
22 W. Lee, M. K. Jin, W. C. Yoo and J. K. Lee, *Langmuir*, 2004, **20**, 7665.
23 X. F. Gao, X. Yan, X. Yao, L. Xu, K. Zhang, J. H. Zhang, B. Yang and L. Jiang, *Adv. Mater.*, 2007, **19**, 2213.
24 M. R. Flynn and J. W. M. Bush, *J. Fluid Mech.*, 2008, **608**, 275.
25 N. J. Shirtcliffe, G. McHale, M. I. Newton, C. C. Perry and F. B. Pyatt, *Appl. Phys. Lett.*, 2006, **89**, 104106.
26 L. Jiang, Y. Zhao and J. Zhai, *Angew. Chem., Int. Ed.*, 2004, **43**(33), 4338–4341.
27 K. Ichimura, S. K. Oh and M. Nakagawa, *Science*, 2000, **288**, 1624.
28 H. Y. Erbil, A. L. Demirel, Y. Avci and O. Mert, *Science*, 2003, **299**, 1377.
29 Z. G. Guo, F. Zhou, J. C. Hao and W. M. Liu, *J. Am. Chem. Soc.*, 2005, **127**, 15670.
30 Z. G. Guo, W. M. Liu and B. L. Su, *Appl. Phys. Lett.*, 2008, **92**, 063104.
31 W. Chen, A. Y. Fadeev, M. C. Hsieh, D. Oner, J. Youngblood and T. J. McCarthy, *Langmuir*, 1999, **15**, 3395.
32 S. R. Coulson, I. Woodward, J. P. S. Badyal, S. A. Brewer and C. Willis, *J. Phys. Chem. B*, 2000, **104**, 8836.
33 D. O. H. Teare, C. G. Spanos, P. Ridley, E. J. Kinmond, V. Roucoules, J. P. S. Badyal, S. A. Brewer, S. Coulson and C. Willis, *Chem. Mater.*, 2002, **14**, 4566.
34 S. A. Brewer and C. R. Willis, *Appl. Surf. Sci.*, 2008, **254**, 6450.
35 A. Nakajima, A. Fujishima, K. Hashimoto and T. Watanabe, *Adv. Mater.*, 1999, **11**, 1365.
36 P. van der Wal and U. Steiner, *Soft Matter*, 2007, **3**, 426.
37 Z. Z. Luo, Z. Z.Z., L. T. Hu, W. M. Liu, Z. G. Guo, H. J. Zhang and W. J. Wang, *Adv. Mater.*, 2008, **20**, 970.
38 N. J. Shirtcliffe, G. McHale, M. I. Newton and C. C. Perry, *Langmuir*, 2003, **19**, 5626.
39 S. H. Li, H. J. Li, X. B. Wang, Y. L. Song, Y. Q. Liu, L. Jiang and D. B. Zhu, *J. Phys. Chem. B*, 2002, **106**, 9274.
40 K. K. S. Lau, J. Bico, K. B. K. Teo, M. Chhowalla, G. A. J. Amaratunga, W. I. Milne, G. H. McKinley and K. K. Gleason, *Nano Lett.*, 2003, **3**, 1701.
41 W. C. Wu, X. L. Wang, D. A. Wang, M. Chen, F. Zhou, W. M. Liu and Q. J. Xue, *Chem. Commun.*, 2009, 1043.
42 D. A. Wang, T. C. Hu, L. T. Hu, B. Yu, Y. Q. Xia, F. Zhou and W. M. Liu, *Adv. Funct. Mater.*, 2009, **19**, 1930.
43 D. Oner and T. J. McCarthy, *Langmuir*, 2000, **16**, 7777.
44 Z. Z. Gu, H. Uetsuka, K. Takahashi, R. Nakajima, H. Onishi, A. Fujishima and O. Sato, *Angew. Chem., Int. Ed.*, 2003, **42**, 894.
45 Z. Yoshimitsu, A. Nakajima, T. Watanabe and K. Hashimoto, *Langmuir*, 2002, **18**, 5818.
46 J. Genzer and K. Efimenko, *Science*, 2000, **290**, 2130.
47 H. Yan, K. Kurogi, H. Mayama and K. Tsujii, *Angew. Chem., Int. Ed.*, 2005, **44**, 3453.
48 X. T. Zhang, O. Sato and A. Fujishima, *Langmuir*, 2004, **20**, 6065.

49 N. J. Shirtcliffe, G. McHale, M. I. Newton, G. Chabrol and C. C. Perry, *Adv. Mater.*, 2004, **16**, 1929.
50 K. Koch, B. Bhushan, Y. C. Jung and W. Barthlott, *Soft Matter*, 2009, **5**, 1386.
51 D. Quere, *Rep. Prog. Phys.*, 2005, **68**, 2495.
52 T. Verho, C. Bower, P. Andrew, S. Franssila, O. Ikkala and R. H. A. Ras, *Adv. Mater.*, 2011, **23**, 673.
53 I. A. Larmour, G. C. Saunders and S. E. J. Bell, *ACS Appl. Mater. Interfaces*, 2010, **2**, 2703.
54 X. J. Liu, W. C. Wu, X. L. Wang, Z. Z. Luo, Y. M. Liang and F. Zhou, *Soft Matter*, 2009, **5**, 3097.
55 W. C. Wu, X. L. Wang, X. J. Liu and F. Zhou, *ACS Appl. Mater. Interfaces*, 2009, **1**, 1656.
56 L. Feng, Y. Zhang, J. Xi, Y. Zhu, N. Wang, F. Xia and L. Jiang, *Langmuir*, 2008, **24**, 4114.
57 M. H. Jin, X. J. Feng, L. Feng, T. L. Sun, J. Zhai, T. J. Li and L. Jiang, *Adv. Mater.*, 2005, **17**, 1977.
58 Z. G. Guo and W. M. Liu, *Appl. Phys. Lett.*, 2007, **90**, 3.
59 Y. K. Lai, C. J. Lin, J. Y. Huang, H. F. Zhuang, L. Sun and T. Nguyen, *Langmuir*, 2008, **24**, 3867.
60 Y. Lai, X. Gao, H. Zhuang, J. Huang, C. Lin and L. Jiang, *Adv. Mater.*, 2009, **21**, 3799.
61 D. Ishii, H. Yabu and M. Shimomura, *Chem. Mater.*, 2009, **21**, 1799.
62 L. Zhai, M. C. Berg, F. C. Cebeci, Y. Kim, J. M. Milwid, M. F. Rubner and R. E. Cohen, *Nano Lett.*, 2006, **6**, 1213.
63 R. P. Garrod, L. G. Harris, W. C. E. Schofield, J. McGettrick, L. J. Ward, D. O. H. Teare and J. P. S. Badyal, *Langmuir*, 2007, **23**, 689.
64 C. Dorrer and J. Ruhe, *Langmuir*, 2008, **24**, 6154.
65 K. Koch, B. Bhushan, H. J. Ensikat and W. Barthlott, *Philos. Trans. R. Soc. London, Ser. A*, 2009, **367**, 1673.
66 X. L. Wang, X. J. Liu, F. Zhou and W. M. Liu, *Chem. Commun.*, 2011, **47**, 2324.
67 B. W. Xin and J. C. Hao, *Chem. Soc. Rev.*, 2010, **39**, 769.
68 K. Ichimura, S. K. Oh and M. Nakagawa, *Science*, 2000, **288**, 1624.
69 B. Zhao, J. S. Moore and D. J. Beebe, *Science*, 2001, **291**, 1023.
70 R. Wang, K. Hashimoto, A. Fujishima, M. Chikuni, E. Kojima, A. Kitamura, M. Shimohigoshi and T. Watanabe, *Nature*, 1997, **388**, 431.
71 N. Sakai, R. Wang, A. Fujishima, T. Watanabe and K. Hashimoto, *Langmuir*, 1998, **14**, 5918.
72 N. Stevens, C. I. Priest, R. Sedev and J. Ralston, *Langmuir*, 2003, **19**, 3272.
73 X. J. Feng, J. Zhai and L. Jiang, *Angew. Chem., Int. Ed.*, 2005, **44**, 5115.
74 R. D. Sun, A. Nakajima, A. Fujishima, T. Watanabe and K. Hashimoto, *J. Phys. Chem. B*, 2001, **105**, 1984.
75 X. J. Feng, L. Feng, M. H. Jin, J. Zhai, L. Jiang and D. B. Zhu, *J. Am. Chem. Soc.*, 2004, **126**, 62.
76 S. T. Wang, X. J. Feng, J. N. Yao and L. Jiang, *Angew. Chem., Int. Ed.*, 2006, **45**, 1264.
77 H. S. Lim, D. Kwak, D. Y. Lee, S. G. Lee and K. Cho, *J. Am. Chem. Soc.*, 2007, **129**, 4128.
78 W. Q. Zhu, X. J. Feng, L. Feng and L. Jiang, *Chem. Commun.*, 2006, 2753.
79 N. Delorme, J. F. Bardeau, A. Bulou and F. Poncin-Epaillard, *Langmuir*, 2005, **21**, 12278.
80 R. Rosario, D. Gust, M. Hayes, F. Jahnke, J. Springer and A. A. Garcia, *Langmuir*, 2002, **18**, 8062.
81 C. G. F. Cooper, J. C. MacDonald, E. Soto and W. G. McGimpsey, *J. Am. Chem. Soc.*, 2004, **126**, 1032.
82 P. F. Driscoll, N. Purohit, N. Wanichacheva, C. R. Lambert and W. G. McGimpsey, *Langmuir*, 2007, **23**, 13181.
83 S. Abbott, J. Ralston, G. Reynolds and R. Hayes, *Langmuir*, 1999, **15**, 8923.
84 S. K. Oh, M. Nakagawa and K. Ichimura, *J. Mater. Chem.*, 2002, **12**, 2262.
85 X. J. Liu, M. R. Cai, Y. M. Liang, F. Zhou and W. M. Liu, *Soft Matter*, 2011, **7**, 3331.
86 H. S. Lim, J. T. Han, D. Kwak, M. H. Jin and K. Cho, *J. Am. Chem. Soc.*, 2006, **128**, 14458.
87 L. Liang, X. D. Feng, J. Liu, P. C. Rieke and G. E. Fryxell, *Macromolecules*, 1998, **31**, 7845.
88 S. Kidoaki, S. Ohya, Y. Nakayama and T. Matsuda, *Langmuir*, 2001, **17**, 2402.
89 H. Yim, M. S. Kent, D. L. Huber, S. Satija, J. Majewski and G. S. Smith, *Macromolecules*, 2003, **36**, 5244.
90 H. Yim, M. S. Kent, S. Mendez, S. S. Balamurugan, S. Balamurugan, G. P. Lopez and S. Satija, *Macromolecules*, 2004, **37**, 1994.
91 T. L. Sun, G. J. Wang, L. Feng, B. Q. Liu, Y. M. Ma, L. Jiang and D. B. Zhu, *Angew. Chem., Int. Ed.*, 2004, **43**, 357.
92 X. J. Liu, Q. A. Ye, B. Yu, Y. M. Liang, W. M. Liu and F. Zhou, *Langmuir*, 2010, **26**, 12377.
93 X. J. Liu, Q. A. Ye, X. W. Song, Y. W. Zhu, X. L. Cao, Y. M. Liang and F. Zhou, *Soft Matter*, 2011, **7**, 515.
94 E. S. Gil and S. A. Hudson, *Prog. Polym. Sci.*, 2004, **29**, 1173.
95 J. X. Wang, J. P. Hu, Y. Q. Wen, Y. L. Song and L. Jiang, *Chem. Mater.*, 2006, **18**, 4984.
96 O. Azzaroni, A. A. Brown and W. T. S. Huck, *Adv. Mater.*, 2007, **19**, 151.
97 F. Zhou, H. Y. Hu, B. Yu, V. L. Osborne, W. T. S. Huck and W. M. Liu, *Anal. Chem.*, 2007, **79**, 176.
98 Y. J. Zhang, Y. F. Shen, J. H. Yuan, D. X. Han, Z. J. Wang, Q. X. Zhang and L. Niu, *Angew. Chem., Int. Ed.*, 2006, **45**, 5867.
99 Y. F. Shen, Y. J. Zhang, Q. X. Zhang, L. Niu, T. Y. You and A. Ivaska, *Chem. Commun.*, 2005, 4193.
100 S. Minko, M. Muller, M. Motornov, M. Nitschke, K. Grundke and M. Stamm, *J. Am. Chem. Soc.*, 2003, **125**, 3896.
101 S. G. Boyes, W. J. Brittain, X. Weng and S. Z. D. Cheng, *Macromolecules*, 2002, **35**, 4960.
102 G. K. Jennings and E. L. Brantley, *Adv. Mater.*, 2004, **16**, 1983.
103 K. S. Liao, H. Fu, A. Wan, J. D. Batteas and D. E. Bergbreiter, *Langmuir*, 2009, **25**, 26.
104 G. Y. Qing and T. L. Sun, *Adv. Mater.*, 2011, **23**, 1615.
105 T. L. Sun and G. Y. Qing, *Adv. Mater.*, 2011, **23**, H57.
106 X. M. Wang, E. Katz and I. Willner, *Electrochem. Commun.*, 2003, **5**, 814.
107 I. S. Choi and Y. S. Chi, *Angew. Chem., Int. Ed.*, 2006, **45**, 4894.
108 J. Lahann, *Science*, 2003, **300**, 903.
109 M. Riskin, B. Basnar, V. I. Chegel, E. Katz, I. Willner, F. Shi and X. Zhang, *J. Am. Chem. Soc.*, 2006, **128**, 1253.
110 E. Katz, O. Lioubashevsky and I. Willner, *J. Am. Chem. Soc.*, 2004, **126**, 15520.
111 J. Isaksson, C. Tengstedt, M. Fahlman, N. Robinson and M. Berggren, *Adv. Mater.*, 2004, **16**, 316.
112 L. B. Xu, W. Chen, A. Mulchandani and Y. S. Yan, *Angew. Chem., Int. Ed.*, 2005, **44**, 6009.
113 T. N. Krupenkin, J. A. Taylor, T. M. Schneider and S. Yang, *Langmuir*, 2004, **20**, 3824.
114 L. B. Zhu, J. W. Xu, Y. H. Xiu, Y. Y. Sun, D. W. Hess and C. P. Wong, *J. Phys. Chem. B*, 2006, **110**, 15945.
115 H. L. Ricks-Laskoski and A. W. Snow, *J. Am. Chem. Soc.*, 2006, **128**, 12402.
116 S. Millefiorini, A. H. Tkaczyk, R. Sedev, J. Efthimiadis and J. Ralston, *J. Am. Chem. Soc.*, 2006, **128**, 3098.
117 Y. S. Nanayakkara, S. Perera, S. Bindiganavale, E. Wanigasekara, H. Moon and D. W. Armstrong, *Anal. Chem.*, 2010, **82**, 3146.
118 R. Rosario, D. Gust, A. A. Garcia, M. Hayes, J. L. Taraci, T. Clement, J. W. Dailey and S. T. Picraux, *J. Phys. Chem. B*, 2004, **108**, 12640.
119 H. Sasaki and M. Shouji, *Chem. Lett.*, 1998, 293.
120 K. Uchida, N. Izumi, S. Sukata, Y. Kojima, S. Nakamura and M. Irie, *Angew. Chem., Int. Ed.*, 2006, **45**, 6470.
121 F. Xia and L. Jiang, *Adv. Mater.*, 2008, **20**, 2842.
122 E. Spruijt, E. Y. Choi and W. T. S. Huck, *Langmuir*, 2008, **24**, 11253.
123 X. M. Wang, Z. Gershman, A. B. Kharitonov, E. Katz and I. Willner, *Langmuir*, 2003, **19**, 5413.
124 Y. F. Zhou, T. Yi, T. C. Li, Z. G. Zhou, F. Y. Li, W. Huang and C. H. Huang, *Chem. Mater.*, 2006, **18**, 2974.
125 B. S. Lee, Y. S. Chi, J. K. Lee, I. S. Choi, C. E. Song, S. K. Namgoong and S. G. Lee, *J. Am. Chem. Soc.*, 2004, **126**, 480.
126 C. Li, R. W. Guo, X. Jiang, S. X. Hu, L. Li, X. Y. Cao, H. Yang, Y. L. Song, Y. M. Ma and L. Jiang, *Adv. Mater.*, 2009, **21**, 4254.
127 D. A. Wang, Y. Liu, X. J. Liu, F. Zhou, W. M. Liu and Q. J. Xue, *Chem. Commun.*, 2009, 7018.

128 D. Wu, S. Z. Wu, Q. D. Chen, Y. L. Zhang, J. Yao, X. Yao, L. G. Niu, J. N. Wang, L. Jiang and H. B. Sun, *Adv. Mater.*, 2011, **23**, 545.
129 L. M. Fidalgo, C. Abell and W. T. S. Huck, *Lab Chip*, 2007, **7**, 984.
130 M. J. Liu, S. T. Wang, Z. X. Wei, Y. L. Song and L. Jiang, *Adv. Mater.*, 2009, **21**, 665.
131 S. R. Coulson, I. S. Woodward, J. P. S. Badyal, S. A. Brewer and C. Willis, *Chem. Mater.*, 2000, **12**, 2031.
132 L. C. Gao and T. J. McCarthy, *J. Am. Chem. Soc.*, 2007, **129**, 3804.
133 K. Tsujii, T. Yamamoto, T. Onda and S. Shibuichi, *Angew. Chem. Int. Edit.*, 1997, **36**, 1011.
134 A. Tuteja, W. Choi, M. L. Ma, J. M. Mabry, S. A. Mazzella, G. C. Rutledge, G. H. McKinley and R. E. Cohen, *Science*, 2007, **318**, 1618.
135 A. Steele, I. Bayer and E. Loth, *Nano Lett.*, 2009, **9**, 501.
136 W. Choi, A. Tuteja, S. Chhatre, J. M. Mabry, R. E. Cohen and G. H. McKinley, *Adv. Mater.*, 2009, **21**, 2190.
137 D. A. Wang, X. L. Wang, X. J. E. Liu and F. Zhou, *J. Phys. Chem. C*, 2010, **114**, 9938.
138 J. P. Zhang and S. Seeger, *Angew. Chem.Int. Ed.*, 2011, **50**, 6652.
139 X. Liu, X. Wang, Y. Liang, S. E. J. Bell, W. Liu and F. Zhou, *Appl. Phys. Lett.*, 2011, **98**, 194102.
140 T. C. Mauldin and M. R. Kessler, *Int. Mater. Rev.*, 2010, **55**, 317.
141 R. P. Wool, *Soft Matter*, 2008, **4**, 400.
142 J. P. Youngblood, N. R. Sottos and C. Extrand, *MRS Bull.*, 2008, **33**, 732.
143 D. Y. Wu, S. Meure and D. Solomon, *Prog. Polym. Sci.*, 2008, **33**, 479.
144 P. Fratzl and R. Weinkamer, *Prog. Mater. Sci.*, 2007, **52**, 1263.
145 A. J. Singer and R. A. F. Clark, *New Engl. J. Med.*, 1999, **341**, 738.
146 Y. Li, L. Li and J. G. Sun, *Angew. Chem. Int. Edit.*, 2010, **49**, 6129.
147 H. J. Li, X. B. Wang, Y. L. Song, Y. Q. Liu, Q. S. Li, L. Jiang and D. B. Zhu, *Angew. Chem. Int. Edit.*, 2001, **40**, 1743.
148 K. S. Toohey, N. R. Sottos, J. A. Lewis, J. S. Moore and S. R. White, *Nat. Mater.*, 2007, **6**, 581.
149 C. J. Hansen, W. Wu, K. S. Toohey, N. R. Sottos, S. R. White and J. A. Lewis, *Adv. Mater.*, 2009, **21**, 4143.
150 H. F. Bohn and W. Federle, *Proc. Nat. Acad. Sci. USA*, 2004, **101**, 14138.
151 T. S. Wong, S. H. Kang, S. K. Y. Tang, E. J. Smythe, B. D. Hatton, A. Grinthal and J. Aizenberg, *Nature*, 2011, **477**, 443.

